

Matter rogue waves

Yu. V. Bludov,¹ V. V. Konotop,^{1,2} and N. Akhmediev³

¹*Centro de Física Teórica e Computacional, Universidade de Lisboa, Complexo Interdisciplinar, Avenida Professor Gama Pinto 2, Lisboa 1649-003, Portugal*

²*Departamento de Física, Universidade de Lisboa, Campo Grande, Edifício C8, Piso 6, Lisboa 1749-016, Portugal*

³*Optical Sciences Group, Research School of Physics and Engineering, The Australian National University, Canberra, ACT 0200, Australia*

(Received 30 June 2009)

We predict the existence of rogue waves in Bose-Einstein condensates either loaded into a parabolic trap or embedded in an optical lattice. In the latter case, rogue waves can be observed in condensates with positive scattering length. They are immensely enhanced by the lattice. Local atomic density may increase up to tens times. We provide the initial conditions necessary for the experimental observation of the phenomenon. Numerical simulations illustrate the process of creation of rogue waves.

DOI: XXXX

PACS number(s): 03.75.Kk, 03.75.Lm, 67.85.Hj

I. INTRODUCTION

Rogue waves are strong wavelets that may appear in the ocean when appropriate conditions are met [1]. These waves can be two, three, or even more times higher than the average wave crests [2]. The resulting peak may reach the height of 20–30 m and by some estimates even 60 m. Clearly, these giants would be very dangerous if it appeared on the path of an ocean liner (and that is why they are also called “killer” waves). Many cases of such encounters are described and even photos are presented [3]. The first measurement of the rogue wave in the open ocean is taken on the oil platform in Norway in 1995 [3], thus confirming that the rogue waves are indeed a reality rather than myths spread by sailors. Detailed studies in the frame of the program “MAXWAVE” that include satellite data showed that waves with the height of 25 m are not unusual [4].

There is a variety of mathematical descriptions of waves in the ocean [5]. One of them, related to deep ocean waves, is based on the nonlinear Schrödinger (NLS) equation [6]. Particular explanations also vary [7]. The basic phenomenon related to this description is Benjamin-Fair (or Bessel-Talanov) [8] instability or more generally speaking modulation instability (MI). Peregrine first noticed that such instability can be responsible for a quick increase in the wave amplitude in the ocean [9]. There is wide range of initial frequencies that are amplified due to MI, and the resulting waves can reach amplitudes substantially higher than those in the initial conditions. In particular, zero-frequency perturbation leads to the wavelet with highest amplitude that is known as Peregrine soliton [9]. The latter is the solution localized in two directions and described analytically by the rational expression [see Eq. (2) below]. Recent studies showed that even higher amplitudes can be reached due to the interaction of several MI components [10] or due to the wavelets that are described by the higher-order rational solution [11].

Recently, the notion of the rogue wave has been transferred into the realm of nonlinear optics [12]. Experimental studies have shown that continuous-wave laser radiation in optical fibers splits into separate pulses and those pulses can

reach very high amplitudes [12]. Indeed, the wave propagation in optical fibers at certain frequencies is described by the NLS equation or its modification, and the nature of appearance of high peaks could be very similar to the peaks in the open ocean. Moreover, due to random modulations of the initial carrier wave in a fiber, the high peaks at the output also arrive randomly just like in the ocean.

There are at least two fundamental reasons for great interest in generating rogue waves in laboratory conditions. First, this opens possibilities for detailed studies of their properties as well as testing applicability of the mathematical models developed for their descriptions (something unthinkable in the natural conditions). Second, being an essentially nonlinear phenomenon, rogue waves allow us to understand deeply the nature and the dynamics of instabilities in nonlinear systems. Thus, the natural question that appears is whether the rogue waves can be observed in other (than ocean or optical fibers) physical media.

The goal of this work is to give the positive answer to this question by showing that rogue waves are also rather natural in the microworld. Namely, they can be observed in Bose-Einstein condensates (BECs). The physical reasons for this are twofold. First, BEC represents a fluid, which in the mean-field approximation is accurately described by the Gross-Pitaevskii (GP), i.e., by the NLS equation [13]. Second, due to the two-body interactions, BEC is intrinsically a nonlinear system. Moreover, a BEC has great advantages compared to other nonlinear systems. Indeed, the nonlinear interactions can be experimentally managed by means of the Feshbach resonance [14], while the effective atomic mass and the stability properties can be varied with help of the optical lattice (OL) [15]. The suitable initial conditions can be created using phase and density engineering. In other words, rogue waves in BECs appear to be well controllable objects.

II. MODEL

To begin with, we start with the one-dimensional (1D) GP equation,

$$i\psi_t = -\psi_{xx} + \sigma|\psi|^2\psi - ig|\psi|^4\psi, \quad (1)$$

94 where $\sigma = \text{sgn}(a_s)$ and a_s is the scattering length. In Eq. (1) 95 we have explicitly included the dissipative term due to in- 96 elastic three-body interaction whose strength is characterized 97 by $g > 0$ [16]. This last point is of special relevance as the 98 rogue waves correspond to a giant increase in the local den- 99 sity when the impact of the three-body collisions can become 100 dominant. 101

102 Besides the inelastic three-body interactions in a real ex- 103 perimental situation relevant for the BEC applications, one 104 has to also take into account a trap potential [see, e.g., the 105 models (4) and (6) below]. This makes the problem very 106 different from the analytically solvable NLS equation. Nev- 107 ertheless, it is natural to expect that using the exact solution 108 for the NLS rogue wave, one can guess the proper initial 109 conditions, giving rise for the giant density enhancement in a 110 realistic mean-field model of a BEC.

111 Therefore, we start by recalling that when $\sigma = -1$ and g 112 $= 0$, Eq. (1) possesses an exact analytic solution [9],

$$\psi_0(x, t) = \rho(x, t)e^{i\theta(x, t)} = \left(1 - 4\frac{1 + 2it}{1 + 2x^2 + 4t^2}\right)e^{it}, \quad (2)$$

114 with the density ρ^2 and the phase distribution θ at each in- 115 stant of time determined directly from this formula. Let us 116 outline the physical properties of the field distribution (2), 117 distinguishing it out of the large class of initial conditions 118 leading to modulational instability. First, we observe that this 119 is a solution with the mean density $n_0 = 1$, in which the do- 120 mains of the high density $n(x, t) \equiv |\psi_0|^2 > 1$ and of the low 121 density $n(x, t) < 1$ are spatially separated at any time, being 122 respectively $|x| < \sqrt{(1+4t^2)}/2$ and $|x| > \sqrt{(1+4t^2)}/2$. Second, 123 the initial amplitude and phase modulation provide that the 124 (superfluid) current density $j(x, t) \equiv i(\psi\bar{\psi}_x - \bar{\psi}\psi_x) = 64xt/(1$ 125 $+ 2x^2 + 4t^2)^2$ is positive (negative) for all $x < 0$ ($x > 0$), i.e., 126 the density excitations move toward (outward) the center x 127 $= 0$ at any instant of time $t < 0$ ($t > 0$). The amplitude of the 128 solution (2) has its maximum at $t = 0$ (see Fig. 1(a)), where 129 the current density is zero $j(0, t) = 0$ at any time.

130 Thus, turning to discussion of possible implementation of 131 the matter rogue waves, we have to look for the initial con- 132 ditions leading to dynamics which would closely resemble 133 the physical behavior described above. While in any experi- 134 ment the time is considered positive, to avoid introducing a 135 time shift in Eq. (2), which would be less convenient for the 136 analytical arguments, we assume that the experiment starts at 137 initial time $t_i < 0$. Moreover, we assume that $|t_i| \gg 1$, i.e., the 138 initial homogeneous density distribution is only weakly 139 modulated. Then the initial condition can be approximated 140 by

$$\rho_i^2 = 1 + \frac{4(2t_i^2 - x^2)}{(2t_i^2 + x^2)^2} \quad \text{and} \quad \theta_i = t_i - \frac{4t_i}{x^2 + 2t_i^2}. \quad (3)$$

142 More generally, this is the case where initially the following 143 properties are satisfied: $\theta_{xx}(x, t_i) \ll \theta_x(x, t_i) \ll \theta_t(x, t_i)$ and, 144 thus, one can neglect the kinetic energy. This readily gives 145 the useful link $\theta_t(x, t_i) \approx \rho^2(x, t_i)$.

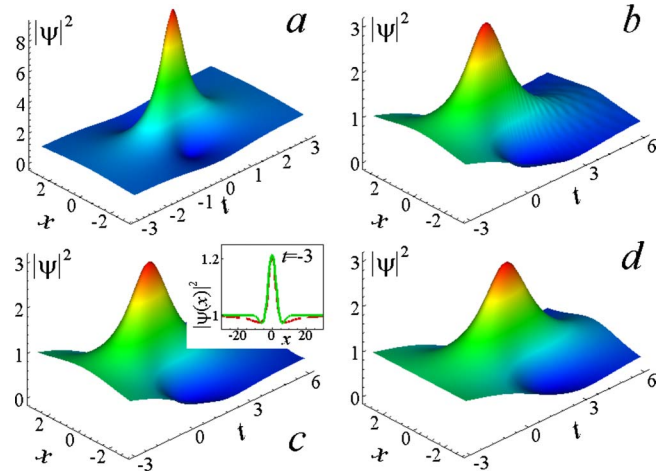


FIG. 1. (Color online) Evolution of the atomic density according to (a) the exact solution (2), (b) TF approximation with $\nu_i = 0.02$, (c) “Mexican hat,” and (d) uniform $\rho_i^2 = 1$ initial conditions. In (b), (c), and (d), the initial phase distribution θ_i is taken from Eq. (3). The initial time is $t_i = -3$. The inset in (c) shows the initial densities obtained from Eq. (2) (dashed line) and from the “Mexican hat” approximation ψ_{MH} (solid line). In (b), (c), and (d), we used $g = 0.05$.

Now, let us consider preparation of the optimal initial 146 conditions for observing rogue waves. We concentrate on the 147 atomic density, assuming that the initial phase distribution θ_i 148 is obtained using the phase imprinting technique [17]. The 149 main difficulty in preparation of the respective initial state 150 arises from the attractive interactions. The latter requires 151 loading the condensate into a modulationally unstable state. 152 Therefore, we take advantage of the Feshbach management 153 [14], allowing one to change abruptly the sign of the scatter- 154 ing length at $t = t_i$. More specifically, at $t < t_i$ we consider 155 the condensate having a positive scattering length, whose abso- 156 lute value could be different from the one exploited in the 157 attractive regime. Thus, we assume that at $t < t_i$ a condensate 158 with $\sigma = \sigma_i > 0$ (generally speaking $\sigma_i \neq 1$) is loaded into a 159 parabolic trap $\nu^2 x^2$, where the dimensionless linear oscillator 160 frequency ν is assumed to be small enough, or more specifi- 161 cally $t_i \nu \ll 1$. In order to create the distribution ρ_i given by 162 Eq. (3), one also has to impose a potential $V_0(x)$ that pro- 163 vides necessary modulations specified below. Then the station- 164 ary state of such BEC is determined from the stationary 165 GP equation 166

$$\mu\psi_i = -\psi_{i,xx} + V_0(x)\psi_i + \nu^2 x^2\psi_i + \sigma_i|\psi_i|^2\psi_i, \quad (4)$$

where μ is the chemical potential. 168

Let us now choose $V_0(x) = \mu - \sigma_i \rho_i^2(x)$. Then $V_0(x)$ is lo- 169 calized on the scale $|x| \lesssim t_i$ as it follows from Eq. (4). Recall- 170 ing that the initial condition we are interested in corresponds 171 to the negligible kinetic energy, we can find ψ_i in the 172 Thomas-Fermi (TF) approximation: $|\psi_{TF}|^2 = \rho_i^2 - \nu_i^2 x^2$. This 173 is valid for $|x| < \bar{x}$, where \bar{x} is the positive zero of $|\psi_{TF}|^2$, and 174 $\nu_i = \nu / \sqrt{\sigma_i}$. Taking into account that at $|t_i| \gg 1$ the distribution 175 $\rho_i \sim 1$, we make the standard estimate $\bar{x} \approx \nu_i^{-1}$. Then the num- 176 ber of atoms loaded into the trap is $\mathcal{N} \approx \int_{-\bar{x}}^{\bar{x}} |\psi_{TF}|^2 dx \sim \frac{4}{3}\bar{x}$. 177

178 Generally speaking experimental creation of the trap po-
179 tential $V_0(x)$ with $\rho_i^2(x)$ given by Eq. (3) can be not easy. It
180 turns out however that excitation of a rogue wave can be
181 implemented using initial distributions, which on the one
182 hand are experimentally feasible and on the other hand
183 closely mimic the “ideal” exact density (3). These case re-
184 quire numerical study, which is performed in the next sec-
185 tion.

186 III. ROGUES WAVES IN HOMOGENEOUS BEC

187 The TF distribution indeed appears to be a good approxi-
188 mation. This is demonstrated by the direct numerical simu-
189 lations shown in Fig. 1 (c.f. the panels a and b). The discrep-
190 ancy between the exact solution ψ_0 and the one generated by
191 ψ_{TF} appears mainly due to the three-body collisions that are
192 not accounted by the exact solution. The remarkable fact is
193 that the rogue wave survives the effect of the quintic dissipa-
194 tive nonlinearity with the latter being responsible only for
195 lowering the maximal amplitude and for retarding times t_m at
196 which the maximum occurs [$t_m \approx 0.5 > 0$ in Fig. 1(b)].

197 This leads us to another issue, namely, the sensitivity of
198 the effect to more general initial conditions. To study this, we
199 consider the example of the “Mexican hat” distribution
200 against the homogeneous background,

$$201 \quad \psi_{MH} = \rho_{MH} e^{i\theta_i}, \quad |\rho_{MH}|^2 = 1 + a \left(1 - \frac{x^2}{\bar{x}^2}\right) e^{-x^2/\bar{x}^2}, \quad (5)$$

202 where θ_i is given by Eq. (3). Such initial conditions can be
203 created by properly adjusted laser beams having the Gauss-
204 ian form. At $\bar{x}^2 \approx 1/2 + 2t_i^2$ and $a = 8/(1 + 4t_i^2)$, the “Mexican
205 hat” distribution well reproduces the desired initial distribu-
206 tion ρ_i given by Eq. (3) [see the inset in Fig. 1(c)]. Figure
207 1(c) shows the dynamics originated by ψ_{MH} . It generates a
208 rogue wave followed by smooth small-amplitude modula-
209 tions of the background.

210 Finally, we have found that the rogue wave can be gener-
211 ated with the help of pure phase engineering, where the ini-
212 tial density is a constant. This scenario is illustrated in Fig.
213 1(d), where θ_i from Eq. (3) was chosen as the initial phase
214 distribution. We again observe the “post-rogue” evolution in
215 the form of the modulated background, which however is
216 slightly different from the previous cases involving density
217 engineering.

218 IV. ROGUE WAVE IN A BEC LOADED IN AN OPTICAL 219 LATTICE

220 Even bigger rogue waves can be observed in a BEC
221 loaded into an OL, where it is developed from the simple
222 Bloch wave. Such a state has two new features. First, the
223 rogue wave is developed on the scale imposed *a priori* and
224 determined by the lattice constant. Second, the phenomenon
225 can be observed in a BEC with a positive scattering length.
226 The latter does not require the use of the Feshbach resonance
227 technique. Analysis presented in the previous section shows
228 that the controlled excitation of the rogue waves requires two
229 conditions to be satisfied simultaneously. These are the re-
230 quirements for the modulational instability as well as special

initial density and velocity distributions. The latter condi- 231
tions can be provided in the case of OL in the same way as 232
for the homogeneous condensate, i.e., using combined den- 233
sity engineering and phase imprinting. The conditions for 234
modulation instability in the case of a BEC loaded in an OL 235
are completely changed by the lattice. The reason is that any 236
two Bloch states bordering different edges of a band gap of 237
the linear spectrum have different stability properties. 238
Namely, one of them is stable while another one is unstable 239
[15]. Thus, for any sign of the scattering length one can 240
achieve the conditions for the modulational instability just 241
choosing correctly one of the initial states. This is the ap- 242
proach which we implemented in this section. 243

To this end, we turn to the GP equation 244

$$i\psi_t = -\psi_{xx} - V \cos(2x)\psi + \sigma|\psi|^2\psi - ig|\psi|^4\psi, \quad (6) \quad 245$$

which now includes a π -periodic OL with the amplitude 246
 $V > 0$. As before, we take into account the inelastic three- 247
body interactions by including the quintic dissipative term. 248
The chosen period of the lattice means that the spatial and 249
temporal variables in Eq. (6) are measured in the units of 250
 d/π and \hbar/E_R , respectively, while the energy is measured in 251
units of the recoil energy $E_R = \hbar^2 \pi^2 / (2md^2)$, where d is the 252
lattice constant and m is the atomic mass. The 1D density 253
distribution $|\psi|^2$ is measured in $\pi^2 a^2 / (4d^2 |a_s|)$ units, where a 254
is the transverse trap width. 255

Let us assume that the initial density is low enough to be 256
well described in the linear approximation with $\sigma = g = 0$. 257
Then, the initial stationary density distribution is nothing else 258
but one of the normalized Bloch states $\varphi_{0,1}(x)$. It is close to 259
one of the energy gaps. We assume that the condensate is 260
loaded into the lowest band, such that the subscripts 0 and 1 261
refer to its minimum (at $q=0$) and to its maximum (at $q=1$), 262
respectively. The wave number q belongs to the first Brill- 263
ouin zone: $|q| \leq 1$. Each Bloch state is characterized by the 264
dispersion relation \mathcal{E}_q and by the effective mass M_q 265
 $= (d^2 \mathcal{E}_q / dq^2)^{-1}$. 266

In the presence of the nonlinearity, one of the Bloch states 267
becomes modulationally unstable [15]. Introducing the non- 268
linearity coefficients $\chi_q = \sigma \int_0^\pi |\varphi_q|^4 dx$, the instability condition 269
can be written down as $M_q \chi_q < 0$. For the chosen initial state, 270
 $M_0 > 0$ and $M_1 < 0$. Hence, for a condensate with a positive 271
 $\chi_{0,1} > 0$ (negative $\chi_{0,1} < 0$) scattering length, the unstable 272
state occurs at the upper, $q=1$ (lower, $q=0$), edge of the first 273
band, i.e., the Bloch state $\varphi_1(x)$ [$\varphi_0(x)$] is unstable. 274

Like in the homogeneous condensates, an excitation of 275
rogue waves in OLs requires an appropriate determination of 276
the initial phase and density distributions. This appears to be 277
easy since the initial state can be of a very low density when 278
it is accurately described within the framework of the 279
multiple-scale approximation. Accordingly, we look for the 280
order parameter in the form $\psi \approx \varepsilon A(\tau, \xi) \varphi_q(x) \exp(-i\mathcal{E}_q t_0)$ 281
(see Ref. [15] for the details), where $q=0,1$, ε is a small 282
parameter discussed below, $\tau = \varepsilon^2 t$, $\xi = \varepsilon x$, and the slowly 283
varying amplitude $A(\tau, \xi)$ solves the NLS equation 284

$$iA_\tau = - (2M_q)^{-1} A_{\xi\xi} + \chi_q |A|^2 A. \quad (7) \quad 285$$

Now, in analogy with Eq. (2), one can construct the exact 286
evolution for A . This, however, will not give us a rogue 287

288 wave, as the giant increase in the density, in a generic case,
 289 breaks the conditions of the applicability of the small-
 290 amplitude approximation. The approximate Eq. (7) however
 291 allows us to determine the proper initial (at $t=t_i$) condition
 292 for exciting rogue waves,

$$293 \quad \psi_i = \frac{\varepsilon}{\sqrt{\chi_q}} \left(1 - 4 \frac{1 - (-1)^q 2i\varepsilon^2 t_i}{1 + 4\varepsilon^4 t_i^2 + 4|M_q| \varepsilon^2 x^2} \right) \\
 294 \quad \times \varphi_q(x) e^{-i[\varepsilon_q + (-1)^q \varepsilon^2] t_i} \quad (8)$$

295 For a given t_i , Eq. (8) contains only one free parameter ε
 296 which determines the scale of the solution. We used smooth
 297 initial modulations with various ε and performed direct nu-
 298 merical simulations of Eq. (6). The results are summarized in
 299 Fig. 2. We observe the emergence of the rogue waves both at
 300 the lower [Fig. 2(a)] and at the upper [Fig. 2(b)] edges of the
 301 first band. The density reaches the values ~ 0.035 , i.e., al-
 302 most 5.5 times higher than the initial amplitude of the modu-
 303 lation. Starting with the higher initial intensity results in the
 304 increase in the rogue wave amplitude by the factor of 15.
 305 This is shown in panels c and d of Fig. 2. Moreover, we can
 306 see that an array of rogue waves is generated. We again
 307 observe that the rogue wave survives the effect of strong
 308 three-body interactions [see Figs. 2(e) and 2(f)].

309 The theory reported above is quasi-1D, while the experi-
 310 mentally created BECs are three dimensional, even in the
 311 cases when cigar-shaped confining potentials are used. This
 312 raises an important question about the validity of this ap-
 313 proximation for the description of rogue waves. More spe-
 314 cifically, we have to establish the conditions which allow one
 315 to describe the condensate in terms of the 1D model even at
 316 the stage of maximal amplitude of the rogue wave. To argue
 317 the applicability of the theory for large regions of the gov-
 318 erning parameters, we recall that, say, in the case of a BEC in
 319 an OL, the transverse dynamics can be neglected only when
 320 the density of the transverse kinetic energy, $\mathcal{E}_\perp = 2d^2/(\pi a)^2$,
 321 is much bigger than both the recoil energy and the energy of
 322 the two-body interactions $\mathcal{E}_{nl} = \max_{x,t} |\psi|^2$ [15] (all measured
 323 in the E_R units). For typical experimental parameters of ^7Li
 324 condensate with $d \sim 1 \mu\text{m}$, $a \sim 0.5 \mu\text{m}$, and $|a_s| \sim 1 \text{ nm}$,
 325 we estimate that $\mathcal{E}_{nl}/\mathcal{E}_\perp \approx 0.044$, 0.38 , and 0.1 in the panels
 326 (a,b), (c,d), and (e,f) of Fig. 2, respectively. Also, the char-
 327 acteristic time of the rogue wave, which we identify with the
 328 time where the density profile significantly exceeds the back-
 329 ground density, can be estimated as $\Delta t \sim 11 \text{ ms}$ (the dimen-
 330 sionless time 500) and $\Delta t \sim 3 \text{ ms}$ (the dimensionless time
 331 140) in panels (a,b) and (c-f) of Fig. 2, correspondingly.
 332 Furthermore, for our numerical simulations the estimate for a
 333 real number of atoms per unit cell is $n = \frac{\pi^2 a^2}{4|a_s|d} |\psi|^2$, i.e., n
 334 $\lesssim 10$. Then the peak density (i.e., the largest number of at-
 335 oms in the central well) is estimated as $n_{peak} \sim 10^2$ [Figs. 2(c)
 336 and 2(d)]. Thus, with suitable choice of the parameters a
 337 rogue wave will neither cause excitation of higher transverse
 338 levels nor break the applicability of the quasi-1D mean-field
 339 approximations (however, neither of these effects is excluded
 340 in principle).

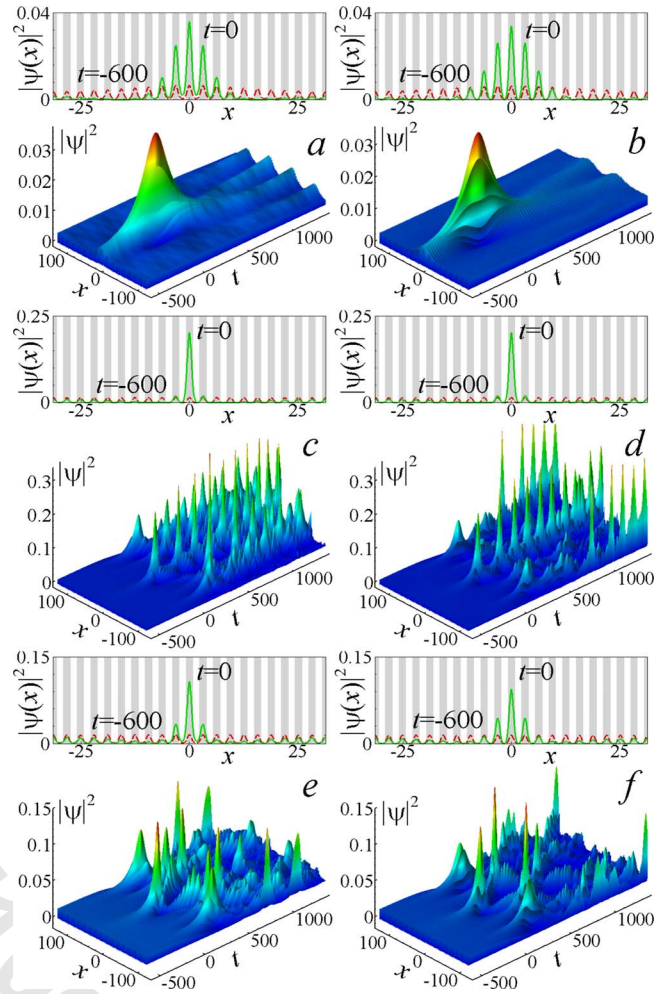


FIG. 2. (Color online) Evolution of the atomic density starting at the lower (left column, $\sigma=-1$, $E_0=-0.9368$) and upper (right column, $\sigma=1$, $E_1=-0.7332$) edges of the first lowest band of the OL with $V=3$. As the initial condition, we used Eq. (8) with $t_i=-600$ and $\varepsilon=0.05$ (panels a,b), $\varepsilon=0.1$ (panels c-f). The rogue wave is observed without dissipative losses (panels a-d) and with inelastic interactions (panels e,f, where $g=0.5$). The upper insets show the respective initial shapes at t_i (dashed lines) and ones at $t=0$, when rogue waves reach their maxima (solid lines) [gray and white strips correspond to half-periods of OL, when $-V \cos(2x) < 0$ and $-V \cos(2x) > 0$, respectively].

V. DISCUSSION AND CONCLUSIONS

341

To conclude, we reported the possibility of observation of
 342 rogue waves in BECs. While the fact that the existence of
 343 such waves is somehow evident, it follows from the fact that
 344 the mean-field dynamics of a BEC is described by the Gross-
 345 Pitaevskii equation; there exists several features of the phe-
 346 nomenon observed in a condensed atomic gas. First, conden-
 347 sates are created in the presence of an external potential,
 348 which is typically parabolic one. Second, the three-body in-
 349 teractions are expected to become a significant factor in the
 350 course of the evolution of the rogue waves (in our simula-
 351 tions they were taken into account by the quintic nonlinearity).
 352 Third, the rogue waves can be generated in a controlled
 353 manner by phase and amplitude engineering.
 354

355 In homogeneous condensates, the rogue waves display lo-
356 cal increase in the amplitude up to several times. The effect
357 can be enhanced using optical lattices due to confining effect
358 of the neighboring lattice maxima. In the latter case, the den-
359 sity amplitude can be amplified tens of times. This occurs on
360 the scale of the lattice constant. The great advantage of the
361 rogue waves in BECs, compared to already observed ones in
362 the ocean and in optical systems, is that they can be manipu-
363 lated using tunable interatomic interactions as well as the
364 flexibility of the confinement and lattice potentials. More-
365 over, the use of the periodic potential allows one to observe
366 rogue waves in media where homogeneous plane waves are
367 stable. The rogue waves are remarkably stable with respect
368 to inelastic three-body interaction. One can further predict
369 that due to giant local increase in the density, the rogue
370 waves can result in enhanced quantum fluctuations, in ap-
371 pearance of the transverse dynamics of the initially quasi-
372 one-dimensional condensate, and even in complete destruc-
373 tion of the atomic condensate.

374 Our study here is devoted to numerical demonstrations of
375 new effects in BEC science. We based our simulations on
376 NLS equation as a rough approximation and confirmed nu-
377 merically that basic rogue wave solution is robust and retains

its features when the equation is perturbed. Clearly, this ap- **378**
 proach raises mathematical questions about stability of rogue **379**
 wave solutions relative to perturbations of the initial equa- **380**
 tion. The preliminary answer is given by our simulations **381**
 using different initial conditions and showing the robustness **382**
 of the rogue waves. As any problem of stability, it is vastly **383**
 complicated and cannot be solved in the frame of a single **384**
 work. Presently, we are at the beginning stage of understand- **385**
 ing these problems, with some results being prepared for a **386**
 separate publication. **387**

Finally, recalling that the modulational instability [15] **388**
 was already observed experimentally [18] and that large di- **389**
 versity of the trap potentials are available experimentally **390**
 [19], the rogue waves appear to be the next exciting phenom- **391**
 enon to look for in future experiments. **392**

ACKNOWLEDGMENTS **393**

Y.V.B. acknowledges support from FCT under Grant No. **394**
 SFRH/PD/20292/2004. The work of N.A. is supported by the **395**
 Australian Research Council (Discovery Project, Grant No. **396**
 DP0985394). **397**

398
399
400

-
- 401** [1] C. Kharif, E. Pelinovsky, and A. Slunyaev, *Rogue Waves in the* **428**
402 *Ocean* (Springer, Heidelberg, 2009). **429**
- 403** [2] A. R. Osborne, *Nonlinear Ocean Waves* (Academic Press, **430**
404 New York, 2009). **431**
- AQ: #05** [3] P. Müller, Ch. Garrett, and A. Osborne, *Oceanogr.* **18**, 66 **432**
2 **406** (2005). **433**
- 407** [4] W. Rosenthal, S. Lehner, H. Dankert, H. Guenther, K. Hessner, **434**
408 J. Horstmann, A. Niedermeier, J. C. Nieto-Borge, J. Schulz- **435**
409 Stellenfleth, and K. Reichert, *Detection of Extreme Single* **436**
410 *Waves and Wave Statistics*, Proceedings of MAXWAVE Final **437**
411 Meeting, October 8–10, 2003, Geneva, Switzerland (unpub- **438**
AQ: #12 lished). **439**
- 3** **413** [5] C. Kharif and E. Pelinovsky, *Eur. J. Mech. B/Fluids* **22**, 603 **440**
414 (2003). **441**
- 415** [6] A. R. Osborne, M. Onorato, and M. Serio, *Phys. Lett. A* **275**, **442**
416 386 (2000); A. R. Osborne, *Mar. Struct.* **14**, 275 (2001). **443**
- 417** [7] P. A. E. M. Janssen, *J. Phys. Oceanogr.* **33**, 863 (2003); V. V. **444**
418 Voronovich, V. I. Shrira, and G. Thomas, *J. Fluid Mech.* **604**, **445**
419 263 (2008); K. B. Dysthe and K. Trulsen, *Phys. Scr.* **T82**, 48 **446**
420 (1999); P. K. Shukla, I. Kourakis, B. Eliasson, M. Marklund, **447**
AQ: #21 and L. Stenflo, *Phys. Rev. Lett.* **97**, 094501 (2006). **448**
- 4** **422** [8] T. B. Benjamin and J. E. Feir, *J. Fluid Mech.* **27**, 417 (1967); **449**
AQ: #23 V. I. Bespalov and V. I. Talanov, *Pis'ma Zh. Eksp. Teor. Fiz.* **3**, **450**
5 **424** 471 (1966); *JETP Lett.* **3**, 307 (1966). **451**
- 425** [9] D. H. Peregrine, *J. Austral. Math. Soc.* **25**, 16 (1983). **452**
- 426** [10] N. Akhmediev, J. M. Soto-Crespo, and A. Ankiewicz, *Phys.* **453**
427 *Lett. A* **373**, 2137 (2009). **454**
- [11] N. Akhmediev, A. Ankiewicz, and M. Taki, *Phys. Lett. A* **373**, **428**
 675 (2009). **429**
- [12] D. R. Solli, C. Ropers, P. Koonath, and B. Jalali, *Nature (Lon-* **430**
don) **450**, 1054 (2007); D.-I. Yeom and B. Eggleton, *ibid.* **431**
450, 953 (2007). **432**
- [13] L. Pitaevskii and S. Stringari, *Bose-Einstein Condensation* **433**
 (Oxford University Press, New York, 2003). **434**
- [14] W. C. Stwalley, *Phys. Rev. Lett.* **37**, 1628 (1976); E. Tiesinga, **435**
 A. J. Moerdijk, B. J. Verhaar, and H. T. C. Stoof, *Phys. Rev. A* **436**
46, R1167 (1992); S. Inouye *et al.*, *Nature (London)* **392**, 151 **437**
 (1998); J. Stenger, S. Inouye, M. R. Andrews, H. J. Miesner, **438**
 D. M. Stamper-Kurn, and W. Ketterle, *Phys. Rev. Lett.* **82**, **439**
 2422 (1999). **440**
- [15] V. V. Konotop and M. Salerno, *Phys. Rev. A* **65**, 021602(R) **441**
 (2002). **442**
- [16] P. O. Fedichev, M. W. Reynolds, and G. V. Shlyapnikov, *Phys.* **443**
Rev. Lett. **77**, 2921 (1996). **444**
- [17] L. Dobrek, M. Gajda, M. Lewenstein, K. Sengstock, G. Birkl, **445**
 and W. Ertmer, *Phys. Rev. A* **60**, R3381 (1999); S. Burger, K. **446**
 Bongs, S. Dettmer, W. Ertmer, K. Sengstock, A. Sanpera, G. V. **447**
 Shlyapnikov, and M. Lewenstein, *Phys. Rev. Lett.* **83**, 5198 **448**
 (1999); J. Denschlag *et al.*, *Science* **287**, 97 (2000). **449**
- [18] L. Fallani, L. De Sarlo, J. E. Lye, M. Modugno, R. Saers, C. **450**
 Fort, and M. Inguscio, *Phys. Rev. Lett.* **93**, 140406 (2004). **451**
- [19] K. Henderson, C. Ryu, C. MacCormick, and M. G. Boshier, **452**
New J. Phys. **11**, 043030 (2009). **453**

AUTHOR QUERIES —

- #1 AU: Units need to be specified for all quantities plotted in figures, unless they are dimensionless. Please check your figures whether any of the quantities plotted has units not specified in the figure, and supply the respective units for inclusion in the figure caption.
- #2 Please verify contents of Ref. 3
- #3 AU: please update Ref. 4 if possible.
- #4 AU: Please check changes to Refs. 7d, 14d, 15, 17a, 17b, and 18.
- #5 Please verify contents of Refs. 8b and 8c